EARTHQUAKE ENGINEERING AND STRUCTURAL DYNAMICS, VOL. 26, 337–359 (1997)

SOIL–PILE–BRIDGE SEISMIC INTERACTION: KINEMATIC AND INERTIAL EFFECTS. PART I: SOFT SOIL

GEORGE MYLONAKIS AND ASPASIA NIKOLAOU
State University of New York at Buffalo, U.S.A.

AND

GEORGE GAZETAS
National Technical University of Athens, Greece

SUMMARY

A substructuring method has been implemented for the seismic analysis of bridge piers founded on vertical piles and pile groups in multi-layered soil. The method reproduces semi-analytically both the kinematic and inertial soil–structure interaction, in a simple realistic way. Vertical S-wave propagation and the pile-to-pile interplay are treated with sufficient rigor, within the realm of equivalent-linear soil behaviour, while a variety of support conditions of the bridge deck on the pier can be studied with the method. Analyses are performed in both frequency and time domains, with the excitation specified at the surface of the outcropping ('elastic') rock. A parameter study explores the role of soil–structure interaction by elucidating, for typical bridge piers founded on soft soil, the key phenomena and parameters associated with the interplay between seismic excitation, soil profile, pile–foundation, and superstructure. Results illustrate the potential errors from ignoring: (i) the radiation damping generated from the oscillating piles, and (ii) the rotational component of motion at the head of the single pile or the pile-group cap. Results are obtained for accelerations of bridge deck and foundation points, as well as for bending moments along the piles.

KEY WORDS: soil; bridge; pier; pile group; pile interaction; radiation damping

INTRODUCTION

Knowledge on the subject of dynamic soil–structure interaction has derived mainly from studies in the last 25 years for buildings and nuclear containment structures on mat foundations.[1–9] The seismic response of pile-supported bridge piers or similar structures has been the subject of considerably smaller research effort.[10–14] The results of such efforts have not yet led to design methods and/or code-type provisions for pile-supported piers, such as the simple methods developed for directly founded structures (Veletsos[4], ATC-3[15]). Therefore, much is yet to be learned on the subject before a complete understanding can develop for the role of crucial problem parameters on the seismic response of pile–bridge systems.

The goals of this paper are: (i) to outline a multi-step equivalent-linear method for analysing efficiently a complete bridge–pier–pile–soil system, emphasising new solutions or improvements over previously published methods (by the senior author and co-workers[14,16–18]); (ii) to present results for two typical bridge–pier systems supported through a single large-diameter drilled pile or a pile group in a moderately soft soil profile, illustrating the role of soil–pile–structure interaction (SPSI) and emphasising the potential errors from some assumptions frequently made in practice. Since the number of the key variables influencing the response is very large, a comprehensive parameter study would be a formidable task, and is certainly beyond the scope of this work.

CCC 0098–8847/97/030337–23

Received 18 October 1995
Revised 23 September 1996

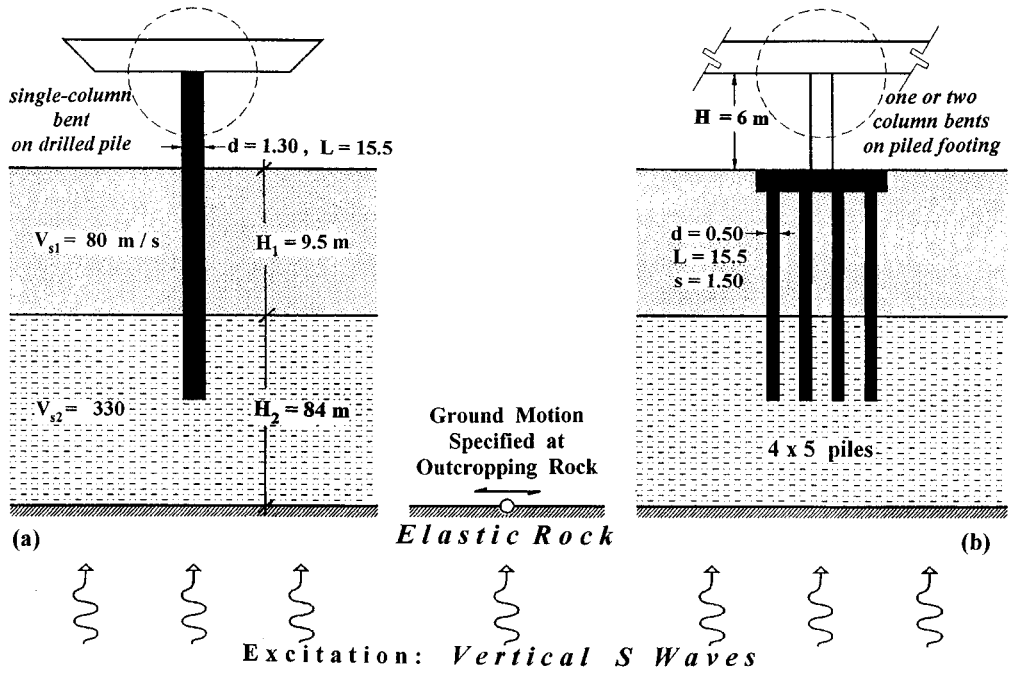

Figure 1. The bridge–pier systems and the soil profile analysed in this paper

THE STUDIED PROBLEM

The two bridge–pier systems analysed in this paper are slightly idealized versions of actual bridges. Portrayed in Figure 1, they involve a single-column bent on drilled pile of the same diameter (d = 1·30 m) and a one- or two-column bent founded on a group of 4 × 5 rigidly-capped d = 0·50 m piles. The height of the column is taken to be 6 m, and the load carried by it 3·5 MN—corresponding roughly to a typical two-lane bridge with spans of about 35 m. Both systems represent widely implemented solutions for highway bridges in many seismically active regions of the world[19,20] and, in fact, several such bridge piers have been damaged in the recent earthquakes of Northridge (1994) and Kobe (1995).

The developed method can handle a variety of realistic pier–bridge–deck support connections, some of which are sketched in Figure 2. They range from a top free to rotate (appropriate for modelling lateral vibrations of relatively long-spanned bridges, or when bridges column and beams are connected through a hinge) to a top fixed against rotation (appropriate for longitudinal vibrations of relatively stiff beams fixed to the column top). Support on elastomeric bearings can also be studied with the method. The results presented herein are for the *fixed* and *free* supports only.

A slightly idealized actual soil profile is considered in this article. Its layering and effective S-wave velocity are depicted in Figure 1, in which the length of the piles (computed with static foundation analysis) is also indicated. This is a type S4 soil (according to NEHRP-1991[21]) or category C (according to EUROCODE-8[22]). Since only ('equivalent') linear analyses are performed herein, the wave velocities shown in Figure 1 are strain-compatible ('effective') quantities. In view of the strong seismic excitation that is presumed to be imposed, this means that the low-strain ('elastic') S-wave velocities would be larger than the shown velocities by a factor of the order of 1·50. This makes the soil profile a typical soft soil stratum. Detailed information on the soil, pile and structural properties used in the analysis is summarized in Table I.

Results are obtained for excitation by vertical S waves, described through a horizontal 'rock' outcrop motion. Both harmonic steady-state and time-history analyses are performed, in the frequency and time

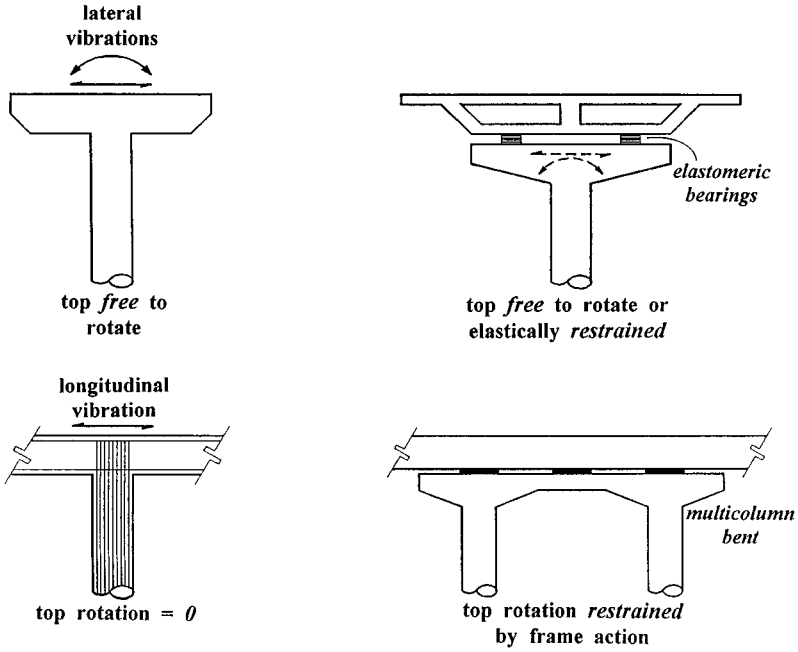

Figure 2. Typical column-deck support connections

Table I. Summary of soil, pile, and structural properties used in the analysis

Soil	Pile	Superstructure
$V_{s1} = 80$ m/s		
$V_{s2} = 330$ m/s	$E = 2{\cdot}5 \times 10^7$ kPa	$E = 2{\cdot}5 \times 10^7$ kPa
$V_{rock} = 1200$ m/s	$d = 1{\cdot}3$ m (single pile)	$I = 0{\cdot}14$ m^4
$\rho_{s1} = 1{\cdot}5$ Mg/m^3	$d = 0{\cdot}5$ m (group pile)	$m_s = 350$ Mg
$\rho_{s2} = 2{\cdot}0$ Mg/m^3	$L = 15{\cdot}5$ m	$H = 6$ m
$\rho_{rock} = 2{\cdot}2$ Mg/m^3	$\rho = 2{\cdot}5$ Mg/m^3	$\beta = 5\%$
$\beta_{s1} = 10\%$		
$\beta_{s2} = 7\%$		

domain, respectively. In the time-domain analyses, two different acceleration histories are used as excitation, both having a peak horizontal acceleration (pga) of about 0·40 g:

(a) an artificial accelerogram approximately 'fitted' to the NEHRP pga = 0·40 g S1-soil elastic response spectrum, or to the Eurocode EC8 soil-category-A spectrum. The 5 per cent damped peak spectral response acceleration for this motion is 1·10 g, i.e. 2·60 times the pga value (compared to 2·50 of the 'target' response spectrum).
(b) the Pacoima downstream accelerogram, recorded recently (on 'soft-rock' outcrop) during the Northridge 1994 earthquake. (Since its pga value is 0·42 g, no scaling of this motion was considered necessary).

The two motions and their 5 and 10 per cent-damped response spectra are plotted in Figure 3. The two ground motions cover a range of possible 'rock' outcrop excitations, necessary for checking the limitations (or showing the generality) of our conclusions. The present article studies the response of bridge structures in

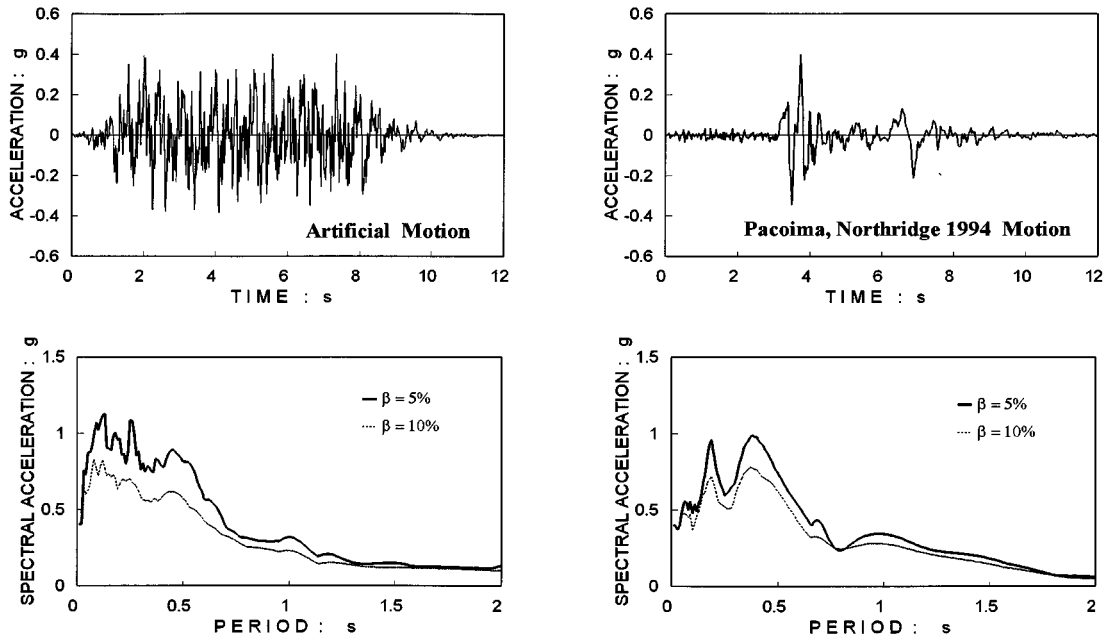

Figure 3. The two 0·40 g motions used in the time-domain analyses, and their 5 and 10 per cent damped response spectra

soft soil. Results for stiffer soil are presented in a companion paper (Part II).[23] A summary of those results can also been found in References 24 and 25.

OUTLINE OF METHOD OF ANALYSIS

The superposition of kinematic and inertial response

The response of bridge–foundation systems such as those of Figure 1 can be computed as the superposition of two effects, as proved by Kausel and Roesset[26] (see also References 9, 27–29): (1) a so-called *kinematic interaction effect* (sometimes also referred to as 'wave scattering' effect), involving the response to base excitation of a hypothetical system which differs from the complete actual system of Figure 1 in that the mass of the superstructure is set equal to zero; (2) an *inertial interaction effect*, referring to the response of the complete pile–soil–structure system to excitation by D'Alembert forces, $-M\ddot{u}_k$, associated with the acceleration, $\ddot{u}_k$, of the superstructure due to the kinematic interaction. This partition is exact for linear soil, pile, and structure if the analysis in both stages is performed rigorously. Nevertheless, as an engineering approximation, the superposition could be applied to moderately non-linear systems. To see how, recall that pile deformations due to lateral loading transmitted from the superstructure attenuate very rapidly with depth (they practically vanish below the 'active' pile length, l_a, which is of the order of 10 pile diameters below the ground surface). Therefore, shear strains induced in the soil due to inertial interaction may be significant only near the ground surface. By contrast, vertical S-waves induce displacements, curvatures and shear strains that are likely to be important only at relatively deep elevations. Thus, since soil strains are controlled by inertial effects near the ground surface and by kinematic effects at greater depths, the superposition may be a reasonable approximation even when non-linear soil behaviour is expected.[9,26,30]

For computational convenience and conceptual simplicity, each one of the above two stages is further subdivided into two independent analysis steps, as follows:

(1) For the *kinematic response*: (*a1*) Analysis of the free-field soil response (i.e. without the presence of piles) to vertically incident S waves; and (*a2*) Analysis of the interaction of the single pile or pile group with

the surrounding soil, driven by the free-field response of step (*a1*). To capture in an (admittedly) crude but simple way the effects of non-linear soil behaviour, different strain-compatible soil moduli can be used for steps (*a1*) and (*a2*).

(2) For the *inertial response*: (*b1*) Computation of the dynamic impedances ('springs' and 'dashpots') at the pile head or the pile-group cap, associated with the swaying ($\mathfrak{R}_x$ and $\mathfrak{R}_y$), rocking $\mathfrak{R}_{ry}$ and $\mathfrak{R}_{rx}$) and cross-swaying-rocking ($\mathfrak{R}_{x,ry}$ and $\mathfrak{R}_{y,rx}$) motion of the foundation; and (*b2*) Analysis of the dynamic response of the superstructure supported on the 'springs' and 'dashpots' of step (*b1*), subjected to the kinematic pile-head motion of step (*a2*). The latter is also called 'Foundation Input Motion (FIM).

For each of the above analysis steps, several alternative formulations have been developed and published in the literature, including finite element, boundary element, semianalytical and analytical solutions, and a variety of simplified methods. Reference is made to Novak,[31] Gazetas *et al*.,[14] and Pender[32] for recent reviews on the subject. In the sequel we only outline some important aspects of each step.

Free-field and single-pile kinematic response analysis

The response to vertical S-wave excitation of a single pile embedded in a layered soil can be obtained numerically in a single step, using a suitable finite-element (FE) formulation with 'wave-transmitting' boundaries (as the one described by Blaney *et al*.[33]), or a boundary-element-type code (as the one described by Mamoon and Banerjee[34]). Instead, a beam-on-Winkler-foundation formulation is used herein. In this, the role of soil-pile interaction is played through a set of continuously distributed *springs* and *dashpots*, the frequency-dependent parameters of which [$k = k(\omega)$ and $c = c(\omega)$] have been calibrated against results of finite-element and boundary-element analyses. Such springs and dashpots connect the pile to the free-field soil; the wave-induced motion of the latter (computed with any available method: e.g., References 35 and 36) serves as the *support excitation* of the pile–soil system.

A frequency-domain method of solution to this problem, presented by Kavvadas and Gazetas,[18] has been extended to the time domain using the Discrete Fourier Transform (DFT) method (see Veletsos and Ventura[37] for a detailed exposition of the method). This can accommodate precisely the frequency dependence of k and c, contrary to methods that require frequency-independent parameters to obtain the response directly in the time domain. It is noted that while such frequency dependence can usually be neglected in single piles, it may be of profound importance in pile groups.[38,39]

In addition, whereas in Reference 18 the problem is solved by forming $4n$ algebraic equations (n = the total number of layers penetrated by the pile) relating pile to free-field displacements (and their first three spatial derivatives), the method used in this work follows a layer transfer matrix approach. This is computationally more efficient, as it involves a sequence of transfer-matrix multiplications and is known in the literature as the Haskell–Thomson or the Holzer method.[40,36,41] Furthermore, the often unrealistic 'rigid bedrock' assumption of that earlier formulation[18] has been eliminated, and the motion can be prescribed at the surface of an outcropping elastic 'rock'.

One of the relative merits of the developed dynamic Winkler method is its versatility in handling approximately moderate levels of non-linearity in the soil surrounding the pile. Such non-linearity arises from the larger stresses induced in the immediate neighbourhood of the pile and could be modelled approximately with a linear analysis of a radially inhomogeneous soil.[42–44] The springs and dashpots resulting from such a (plane-strain) analysis would reflect the non-linearities due to pile–soil interaction, rather than the (additional) non-linearities due to shear waves propagating in the free field soil.

The computational advantages of the Winkler-based ('Beam-on-Dynamic-Winkler-Foundation' or BDWF) method over the aforementioned numerical methods can hardly be overstated. At the same time, the results of BDWF are in full accord with those of the more rigorous methods—not surprising in view of the approximate validity of the main assumptions of the model[31,45] and the calibration at the layer level of the former with the results of the latter. As an example, Figure 4 illustrates a typical good comparison for kinematic displacements and bending moments in a pile embedded in a shorter version ($H_2 = 20{\cdot}5$ m) of the studied soft soil profile, computed with the two methods (BDWF and FEM).

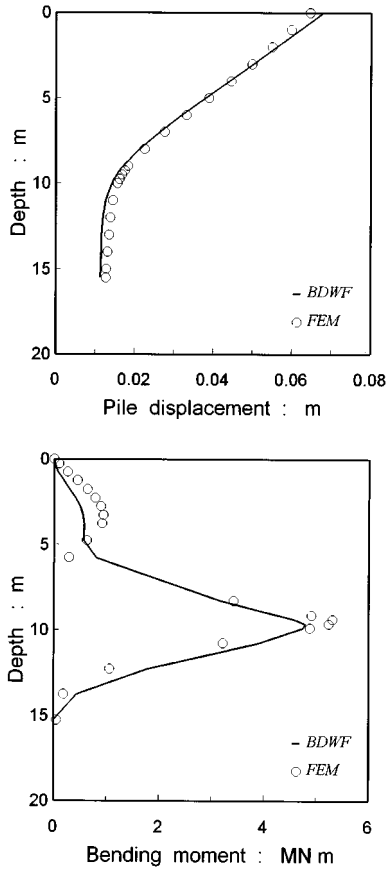

Figure 4. Comparison between kinematic steady-state displacement and bending moment diagrams, computed with a rigorous finite element [33] and dynamic Winkler model (BDWF) at $T = 0{\cdot}52$ s for a pile embedded in the soil profile of Figure 1 with $H_2 = 20{\cdot}5$ m

It has been found that the kinematic interaction between pile and soil has, in general, two consequences:[18,38,46]

(i) It filters out low-period components of the motion while at the same time it induces a rotational component at the pile head
(ii) it induces axial, bending, and shear deformation on piles. Bending is significant at two locations: at the top of fixed-head piles and at the interfaces of soil layers with sharply different stiffnesses.

Dynamic impedances for single pile

The dynamic response of a head-loaded pile has been studied in the literature far more extensively than the kinematic pile response to seismic wave excitation. Two recent state-of-the-art papers, by Novak[31] and by Pender,[32] provide comprehensive information on the subject. Much of the published work has modelled the soil as a continuum and developed numerical and (semi) analytical methods to derive the dynamic impedances (i.e. force to displacement ratios) $\mathfrak{R}$ at pile head, in the form

$$\mathfrak{R} = K + \mathrm{i}\omega C \tag{1}$$

where $K = K(\omega)$ denotes the dynamic stiffness and $C = C(\omega)$ the dashpot parameter; the latter reflects both radiation (geometric) and hysteretic (material) damping in the system. Winkler-type models have also been developed, following the original work by Novak.[47]

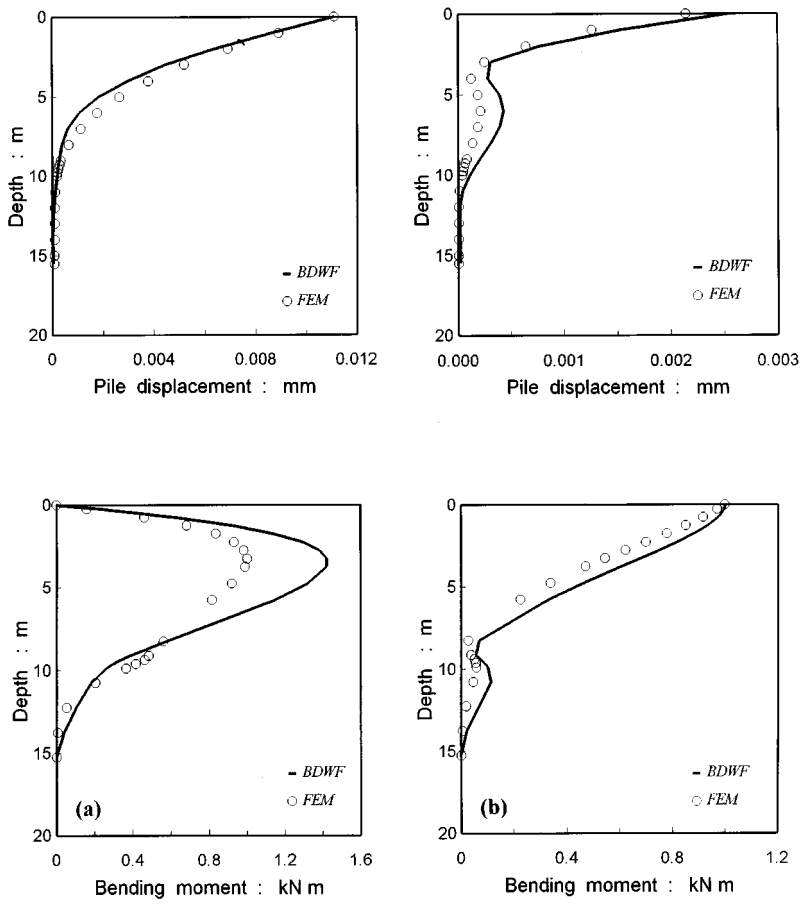

Figure 5. Comparison between inertial steady-state displacement and bending moment diagrams, computed with a rigorous finite element (Blaney et al.[33]) and dynamic Winkler model (BDWF) at $T = 0{\cdot}52$ s for: (a) a unit force and (b) a unit moment atop the pile of Figure 1(a)

The results of such studies have been utilized by several researchers in developing simple algebraic expressions for directly estimating the dynamic impedances of single piles in some idealized (homogeneous and inhomogeneous) soil profiles.[48] On the other hand, the information published to date for the dynamic internal forces (bending moments and shear forces) developing in a head-loaded pile is scarce.

In this work, use is made of a Beam-on-Dynamic-Winkler-Foundation (BDWF) formulation, analogous to the one described in the previous section for the kinematic response, but with the supports of the springs and dashpots fixed in space and the loading applied at the top.

In addition to its versatility, the developed Winkler model leads to results in accord with those of more rigorous methods, as illustrated in Figure 5. Moreover, soil nonlinearity near the top can be taken into account by using effective soil moduli that are only a fraction of the low-strain ('maximum') soil moduli.

Pile-to-pile interaction

The dynamic impedance of a group of piles in any mode of vibration cannot be computed by simply adding the stiffnesses of the individual piles, since each pile is affected not only by its own load, but also by the load and deflection of the neighbouring piles. Similarly, the seismic response of a pile group may differ from the response of each individual pile taken alone, because of additional deformations transmitted from the adjacent piles. This pile-to-pile interaction is frequency-dependent, resulting from waves that are emitted

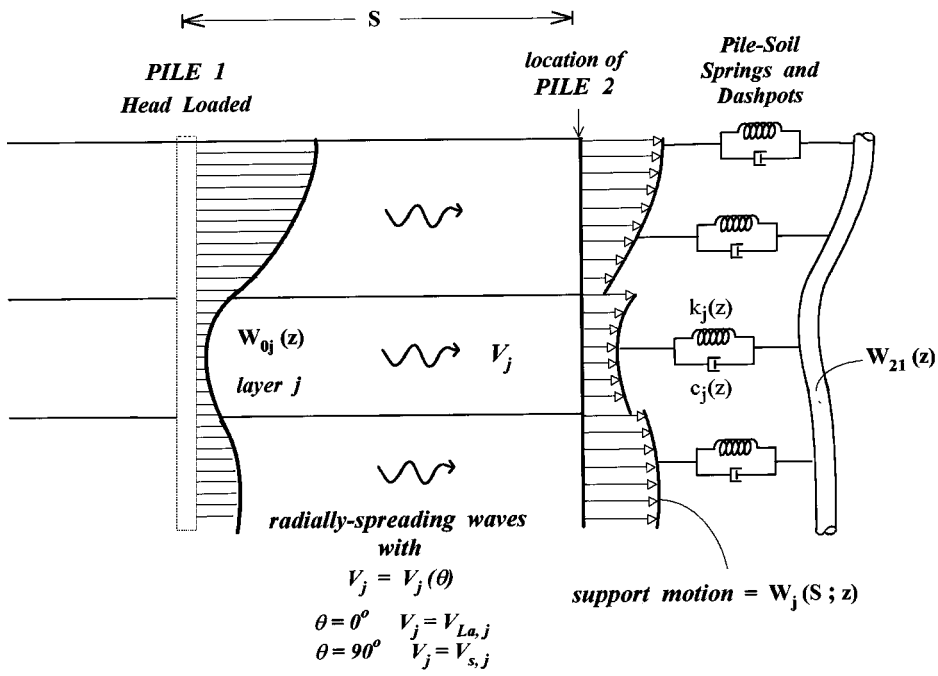

Figure 6. Schematic illustration of the wave interference method for computing the influence of the harmonically head-loaded 'active' Pile1 upon the adjacent 'passive' Pile2, in a layered soil[54]

from the periphery of each pile and propagate to 'strike' the neighbouring piles. A variety of numerical and analytical methods have been developed to compute the dynamic response of pile groups accounting for pile-to-pile interaction. Makris and Gazetas[16] have shown that this group effect is of profound importance *only for head-loaded piles*. For kinematic seismic loading the group effect could for all practical purposes be neglected.

To determine the group impedances, use is made of Poulos' superposition approach, extended to dynamic loading by Kaynia[38] and Sanchez-Salinero.[49] Frequency-dependent *interaction factors*, i.e. displacement ratios expressing the effect of one pile onto another, are a key ingredient of the method. Such factors have been derived using rigorous boundary-element-type methods.[38,50] For a homogeneous soil in particular, a simple analytical solution proved possible: to this end Dobry and Gazetas[39] and Makris and Gazetas[16] considered the cylindrical waves emanating from all points along the pile periphery and, after some attenuation, striking the neighbouring pile. Using simple wave propagation theory, this leads closed-form expressions for each of the principal (horizontal and vertical) modes of deformation. This simple theory (termed '*wave interference*' solution by Wolf[51]) is in very good accord with rigorous methods.[39,51,32]

Soil layering, however, has been found to affect substantially pile-to-pile interaction factors. For example, in the presence of a stiff soil layer (or of rock) at the pile base (tip), the *vertical* interaction factors (which control both vertical and rocking oscillations) would decrease to only a small fraction of the values computed for piles 'floating' in homogeneous half space.

For a number of layered and inhomogeneous soil profiles, complete sets of interaction factors are now available in the form of ready-to-use non-dimensional graphs.[52,53] Moreover, the aforementioned simple '*wave interference*' method[39,16] can be extended to a layered soil profile. To this end, Mylonakis[54] considers (as sketched in Figure 6) that the cylindrical waves are emitted from the periphery of the 'active' pile with a different amplitude W_{0j} and phase angle ϕ_{0j} in each soil layer j. Radial spreading of these waves leads to

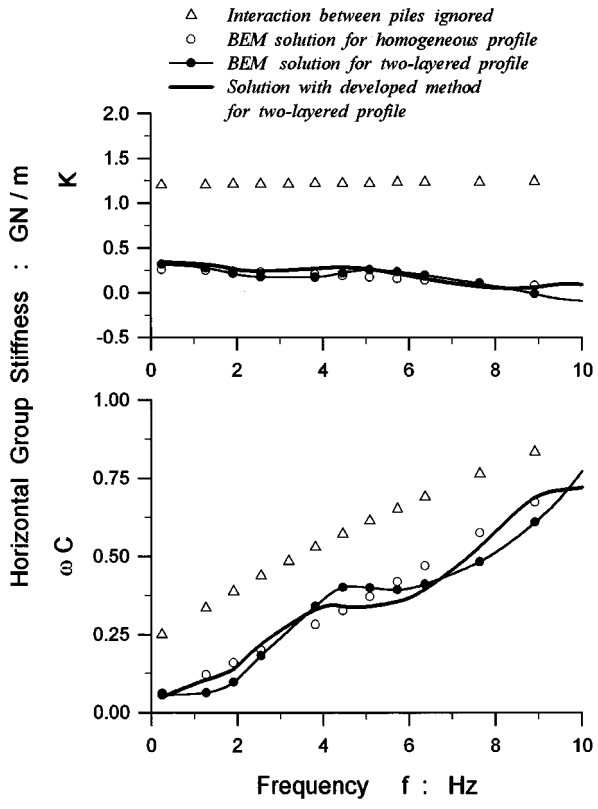

Figure 7. Dynamic horizontal stiffness (in the longitudinal 5-pile direction) for the 4×5 pile group embedded in the 'Soft Clay' profile. Comparison of rigorous Boundary Element[38] and the simplified developed method. Notice the errors from ignoring pile-to-pile interaction

(different for each layer) attenuation and change in phase, in accordance with

$$W_j(S) \approx W_{0j} \sqrt{\frac{r_0}{S}}\, e^{-(i+\beta_j)\omega(S-r_0)/V_j} \tag{2}$$

where S is the radial distance of interest r_0 the pile radius; $i = \sqrt{-1}$; β_j hysteretic soil damping ratio; and V_j the appropriate wave propagation velocity for layer j. For vertical and rocking oscillations: $V_j = V_{sj}$ (the S-wave velocity); but for lateral oscillation V_j depends on the direction of loading with respect to the line connecting the two piles. Specifically: $V_j = V_{sj}$ if the piles are off-line (at $\theta = 90^\circ$ with respect to the direction of loading), or $V_j = V_{Laj}$ (the so-called 'Lysmer's analog' velocity[39]) if the piles are in-line (at $\theta = 0^\circ$ with the direction of loading). For angles θ between 0° and 90° interpolation is done as described in References 38 and 39.

The effect of the arriving waves $W_j(S)$ on a second ('passive') pile loaded at a distance S is computed by considering $W_j(S)$ as the support motion of this pile, as was done for a homogeneous profile.[16] Details can be found in the dissertation of Mylonakis.[54] The interaction factor, α, is defined as the ratio of the top displacements of the 'passive' and 'active' pile: $W_{21}(0)/W_{01}(0)$.

For the aforementioned 4×5 pile group in the two-layer soil Profile of Figure 1, Figure 7 compares the dynamic horizontal, stiffnesses (real and imaginary parts) of the group computed with the above-outlined method and with a rigorous boundary-element-type formulation.[38] Notice the generally good agreement between the two methods. Also plotted in this figure are (i) the corresponding solution for a homogeneous half space having the properties of the top clay layer, and (ii) the impedance (stiffness and damping) functions

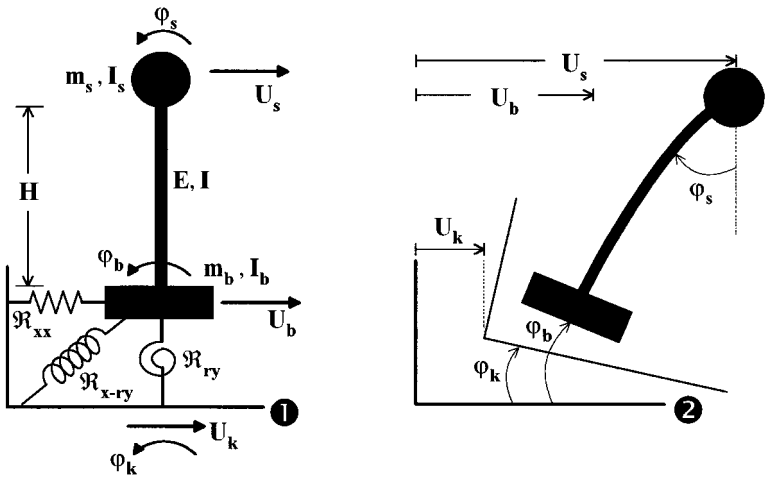

Figure 8. The model for the analysis of soil–structure interaction: (1) model parameters and notation and (2) sketch of response in terms of absolute displacements and rotations

of the group if pile-to-pile interaction were completely ignored. Notice the substantial overprediction of both impedances in this case.

Seismic response of the bridge pier

Having determined: (i) the two components (translation U_k and rotation φ_k) of the kinematic response of the foundation, (i.e. the 'Foundation Input Motion'), and (ii) the pile-group dynamic impedances $\Re_{ij}$, the response of the bridge–pier, namely the (absolute) displacement and rotation of the pier top (deck) and bottom (pile cap), can be computed from (Figure 8)

$$\begin{Bmatrix} U_s \\ \varphi_s \\ U_b \\ \varphi_b \end{Bmatrix} = ([K] - \omega^2[m])^{-1} \begin{Bmatrix} 0 \\ 0 \\ [\Re_{ij}] \begin{Bmatrix} U_k \\ \varphi_k \end{Bmatrix} \end{Bmatrix} \tag{3a}$$

where

$$[K] = \begin{bmatrix} [K_{ss}] & [K_{sb}] \\ [K_{bs}] & [K_{bb}] + [\Re_{ij}] \end{bmatrix} \tag{3b}$$

$$[m] = \begin{bmatrix} [m_{ss}] & [0] \\ [0] & [m_{bb}] \end{bmatrix} \tag{3c}$$

where $[K_{ss}]$, $[K_{sb}]$, $[K_{bs}]$ and $[K_{bb}]$ are the four stiffness submatrices corresponding to the superstructure (s) and its base (b)$_j$ $[m_{ss}]$, $[m_{bb}]$ are the mass-submatrices of the superstructure and the foundation, respectively (see References 8 and 54).

Having computed the response of the superstructure, all the remaining response variables such as pile displacements, bending moments and shear forces can be readily obtained. All the above quantities are calculated in a complex-valued frequency domain form. It is then straightforward to obtain time-history response functions, corresponding to a specific earthquake excitation, by using the aforementioned DFT technique.

Table II. The eight cases studied in the paper: A1, A3, A4, C1, C3, C4, A21, C21

Bridge–foundation systems	Rock-outcrop excitation	Nature of analysis approximations
Single column-pile (case A)	Harmonic	*case 1**: complete analysis ('exact') *case 21***: complete analysis ('exact')
Single column on 4×5 pile group (case C)	Artificial	*case 3**: pile cap fixed against rotation
	Pacoima 1994	*case 4**: pile radiation damping = 0

* no rotation at column top ** column top free to rotate

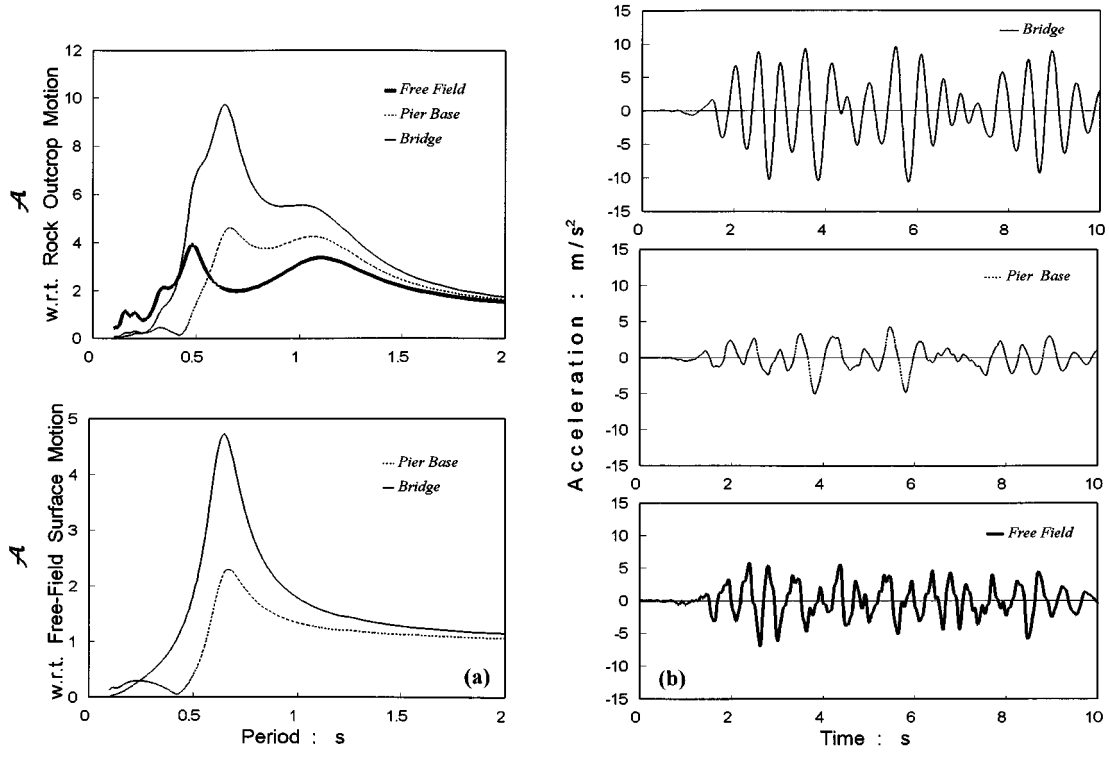

Figure 9. Case A1, no rotation at the column top: results of the complete analysis in terms of: (a) harmonic steady-state transfer functions and (b) response acceleration histories for the artificial excitation

PARAMETRIC RESULTS

Table II summarizes the types of dynamic analysis performed for the two bridge–pier systems of Figure 1. In most cases all three types of ground motion were used as excitation: harmonic (steady-state), artificial time-history, Pacoima-downstream accelerogram. However, only in a few selected cases are the results shown for all motions.

The results are portrayed in Figures 9, 11 and 15–19 in two parts. Part (a) shows non-dimensional steady-state transfer functions, $\mathscr{A}(T)$, relating bridge and foundation response amplitudes to the rock outcrop and free field motion amplitudes; $\mathscr{A}$ are ratios between either displacements or accelerations. Part (b) shows acceleration time-histories of the bridge, foundation, and free-field for the artificial accelerogram

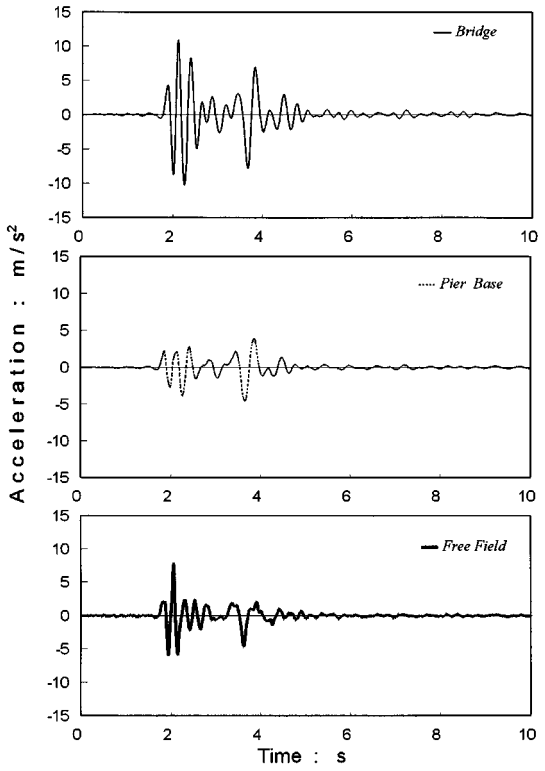

Figure 10. Case A1, no rotation at the column top: results of the complete analysis in terms of response acceleration histories for the Pacoima (1994) downstream motion

applied at the rock outcrop. Figure 10 is similar to Figure 9(b) but for the Pacoima excitation; although comments on the response to the Pacoima excitation under other conditions will be given later, only Figure 10 gives graphical output for this excitation.

In addition, steady-state amplitudes and peak values of bending moments in the pile are given in Figures 12–14. Figures 15–19 have the same format as Figures 9 and 11 with divisions into parts (a) and (b), but for different assumptions.

Complete analysis: *the case of no rotation at column top*

Case A1 and C1, correspond to the (most) complete analyses of the two pier systems of Figure 1, with the top of their column considered rigidly connected to a non-rotating deck. The results are portrayed in Figures 9–11. The following noteworthy observations can be made with the help of these figures:

(1) The fundamental natural period, T_1, of the whole soil deposit appears to be about 1·1 s. As it can be easily checked, the response at this period is largely dominated by the characteristics of the thick-and-stiff lower sandy layer (S-wave velocity 330 m/s, thickness 83.5 m, corresponding period: $4H/V_s = 4 \times 83{\cdot}5/330 \approx 1$ s $\approx T_1$). The relatively small 'impedance' contrast, I_R, between this layer and the underlain soft rock:

$$I_R = \frac{\rho_r V_r}{\rho_{s2} V_{s2}} = \frac{2{\cdot}2 \times 1200}{2 \times 330} \approx 4 \tag{4}$$

generates sufficient radiation damping to reduce the soil amplification at this period to a mere 3.3. One could have expected such a low value at resonance, on the basis of Roesset's simple one-layer

formula:[36,55]

$$\mathscr{A}_1 \approx \frac{1}{(\pi/2)\,\beta_{s2} + (I_R)^{-1}} = \frac{1}{(\pi/2)(0{\cdot}07) + 1/4} \approx 2{\cdot}8 \tag{5}$$

The second natural period, T_2, of the soil deposit appears to equal almost 0·5 s and the respective amplification, $\mathscr{A}_2$, is nearly 4—a rather substantial value for a *second-mode* resonance. Apparently, this mode is dominated by the characteristics of the top clay layer: natural period of the top layer $= 4H/V_s = 4 \times 9{\cdot}5/80 \approx 0{\cdot}48$ s $\approx T_2$). The relatively high amplification reflects the smaller radiation into the underlain stiff soil layer, due to the now larger 'impedance' contrast:

$$I'_R = \frac{2 \times 330}{1{\cdot}5 \times 80} \approx 5{\cdot}5 \tag{6}$$

compared to $I_R \approx 4$ between the second layer and underlying base.

(2) For the response of the bridge pier A (single column-pile), the role of the second resonance in the soil is much more significant than the first, for two reasons: *First*, the fundamental natural period of the pier–foundation–soil system $\tilde{T}$, is about 0·65 s—much closer to T_2 (0·5 s) than to T_1 (1·1 s); hence, the amplitude increase and broadening of the bridge amplification curve (with respect to rock outcrop) at resonance. *Second*, in the time domain, the response spectra of both rock excitations (recall Figure 3) show that most of the incident seismic energy is carried by harmonic components with periods smaller than or about equal to 0·5 s. This is, in fact, the usual case with 'rock' motions. For periods exceeding by far 0·5 s (e.g. $T = T_1 \approx 1{\cdot}1$ s) the input motion is too weak to produce a substantial soil or structure response, despite the unquestionable amplification by a factor $\mathscr{A}_1 \approx 3{\cdot}3$. As a result, the bridge acceleration histories show a prevailing period of about 0·60 s, with hardly an evidence of a role for the fundamental period, $T_1 = 1{\cdot}1$ s, of the deposit.

(3) The fundamental period, $\tilde{T}$, of the pier-foundation–soil system for bridge pier C (single column on 4×5 piles) appears from Figure 11 to equal about 0·37 s. This is quite close to the fixed-based fundamental period of the superstructure:

$$T_{st} = 2\pi \sqrt{\frac{m_s}{12EI/H^3}} \approx 0{\cdot}27 \text{ s} \tag{7}$$

This proximity of periods for pier C($\tilde{T}/T_{st} = 0{\cdot}37/0{\cdot}27 \approx 1{\cdot}3$ as opposed to $0{\cdot}65/0{\cdot}27 \approx 2{\cdot}41$ for pier A) stems of course from the presence in this case (C) of the group of twenty 0·50 m diameter piles, the rotational stiffness of which is an-order-of-magnitude larger than of the 1·30 m diameter single pile of pier A.[24]

Extending the arguments of earlier paragraphs in this section, it is seen that in this case the role of the fundamental soil period, $T_1 = 1{\cdot}1$ s, is even less significant (compare the bridge transfer functions with respect to rock at $T = T_1$: $A \approx 3{\cdot}8$ for pier C versus $A \approx 5{\cdot}3$ for pier A). The second natural soil period, $T_2 \approx 0{\cdot}50$ s, increases in importance as is evident from the fact that at this period the transfer functions of both bridge and pile cap exhibit their largest peaks.

In addition, the two dominant periods of the system in this case, 0·35 and 0·50 s, fall within or very close to the range of dominant periods of the rock accelerograms. Consequence: the response acceleration peaks at both bridge-deck and pile-cap elevations (1·40 and 0·80 g, respectively) exceed those of pier A (1·10 and 0·60 g, respectively).

(4) The response of the head of the single pile of pier A shows a somewhat different behaviour than the response of the bridge deck. The pile-cap transfer function (with respect to the rock excitation) does not exhibit any tendency to increase at $T = T_2 \approx 0{\cdot}5$ s, as is the case with the bridge deck. The two peaks in this transfer function, corresponding to periods T_1 and $\tilde{T}$, are of nearly equal value, $\mathscr{A} \approx 4$. They represent the kinematic and inertial response peaks, respectively.

This can be further illustrated by examining the (steady-state) bending moments developing in the pile for periods $T = T_1$, $T = \tilde{T}$ and $T = T_2$ (Figure 12). It becomes evident that the first period (T_1)

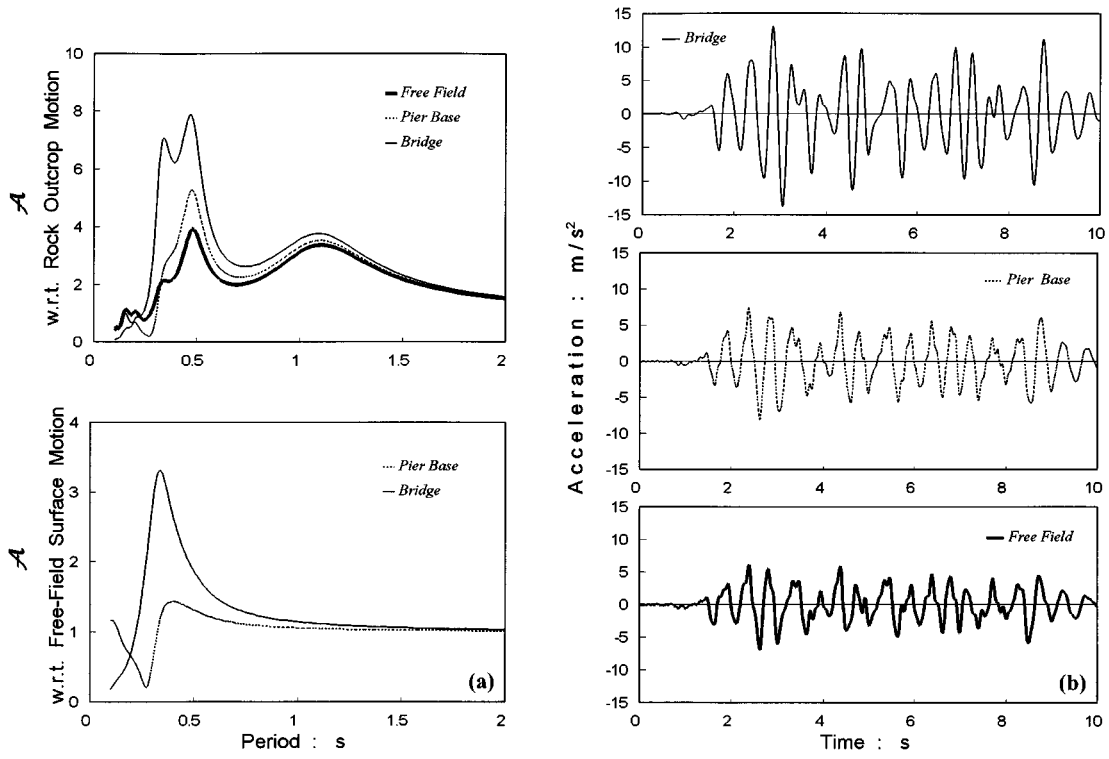

Figure 11. Case C1, no rotation at the column top: results of the complete analysis in terms of: (a) harmonic steady-state transfer functions and (b) response acceleration histories for the artificial excitation

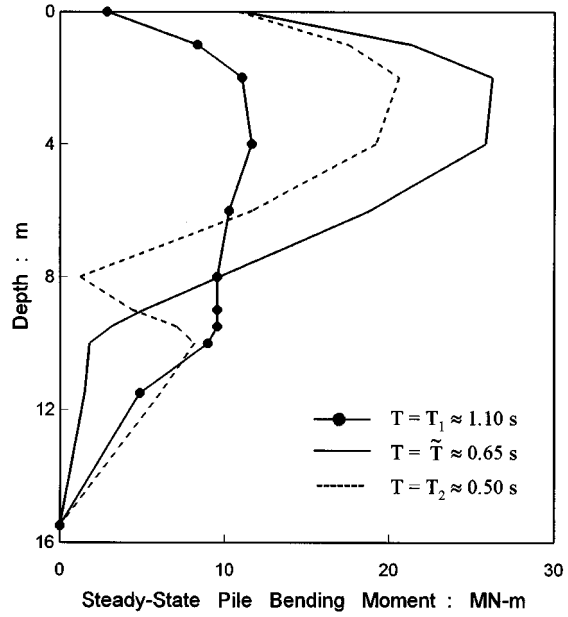

Figure 12. Case A1, no rotation at the column top: steady-state pile bending moment diagram for $T = T_1$ (fundamental period of the deposit), $T = T_2$ (second period of the deposit), and $T = \tilde{T}$ (fundamental period of the pier–foundation–soil system)

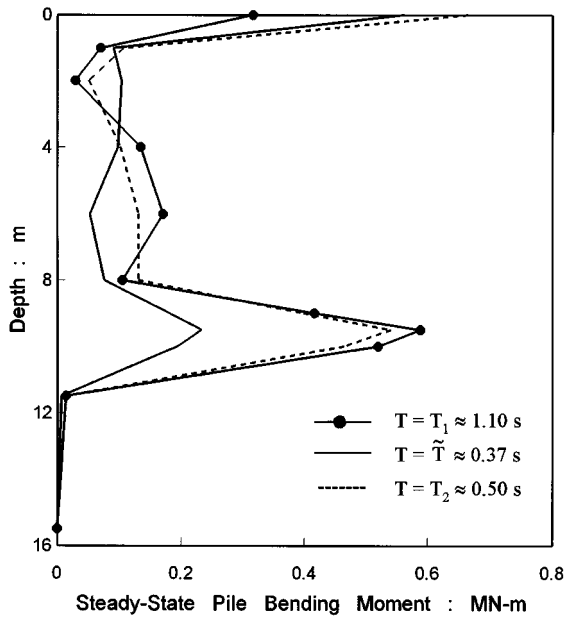

Figure 13. Case C1, no rotation at the column top. Steady-state pile bending moment for $T = T_1$ (fundamental period of the deposit), $T = T_2$ (second period of the deposit), and $T = \tilde{T}$ (fundamental period of the pier–foundation–soil system)

controls the largest moment in the clay-sand interface (a clearly kinematic effect) while $\tilde{T}$ controls the largest moment in the clay-stand interface (a clearly kinematic effect) while $\tilde{T}$ controls the largest moment at the upper part of the pile (an inertial effect). At $T = T_2$ the bending moment diagram has similarities with both of the above diagrams: near the layer interface it nearly reaches the values of the $T = T_1$ diagram (evidence of kinematic response); near the top it is similar to the $T = \tilde{T}$ diagram (evidence of inertial response).

An important conclusion from Figure 12 is that, in this case of a pier on a single pile, the inertial bending moments in the upper half of the pile exceed significantly the kinematic moments at, and near the interface. The reason for this is that the inertial force developed on the bridge deck is directly transmitted as a shear force and bending moment onto the head of the pile. At resonance, $T = \tilde{T}$, this inertial force is large and so is therefore the imposed moment on the pile.

(5) The above picture is not exactly valid for the response of the pile cap of pier C (Figure 11). At $T = T_2 \approx 0{\cdot}5$ s both the bridge deck and the pile cap exhibit a strong peak in their transfer functions (with respect to rock), similar with the peak in the free-field soil amplification curve. This is apparently the result of a '*constructive interplay*' *between the soil in resonance and the structure in near-resonance.*

The distribution with depth of steady-state bending moments at $T = T_1$, $\tilde{T}$, and T_2 is plotted in Figure 13. Again, the largest *kinematically driven* moment at the interface occurs at $T = T_1$ and is nearly matched by the moment at $T = T_2$. The largest *inertia-driven* moment at and near the top occurs at $T = T_2$ (for the reasons explained in the preceding paragraph) and is essentially matched by the moment at $T = \tilde{T}$. Notice that in this case the moments at the interface are about the same as the moment at the top. This is because the overturning moment produced by the bridge deck inertia is now resisted mainly by axial pile compression–extension rather than bending of the piles. The time-domain peak values of the bending moments plotted for these two cases in Figure 14, also reflect the above trends.

It may be of engineering interest to take note of the peak values of bending moments in the 1·30 m diameter pile (about 8 MN m) and in the 0·50 m diameter pile (about 0·3 MN m). Developing during strong seismic excitation (pga $\approx$ 0·4 g at rock outcrop), these moments could be resisted by a properly reinforced concrete cross-section at about its yield capacity.

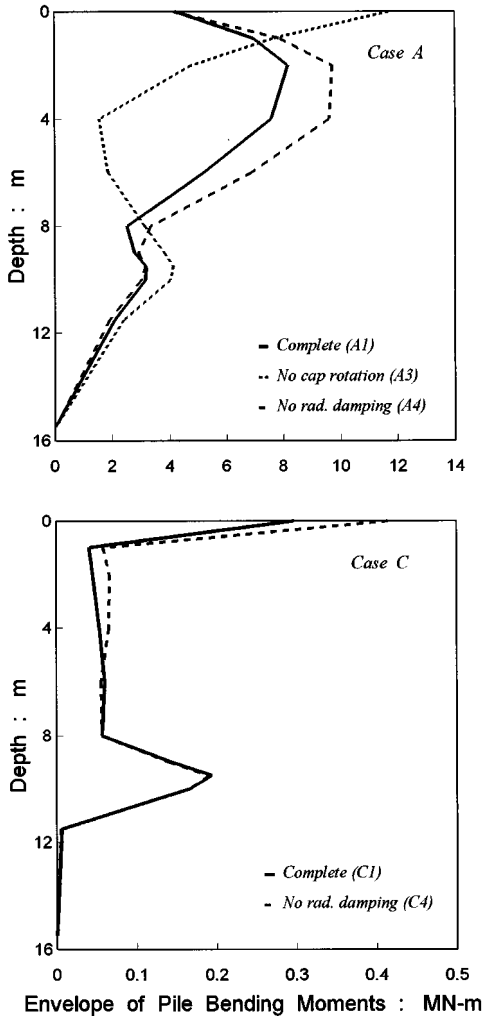

Figure 14. Envelopes of peak values of bending moments along the single pile of pier A (case A1, A3, A4) and the corner pile of the pile group of pier C (cases C1, C4) for the artificial excitation

Complete analysis: the case of free-to-rotate column top

Cases A21 and C21 differ from A1 and C1, respectively, only in that the column top and the supported bridge deck are free to rotate.*

The steady-state transfer functions plotted in Figures 15 and 16 reveal that the response is now dominated to a greater extent by the characteristics of the structure. In each of the two figures there is essentially only one significant resonant peak; it occurs at the fundamental period $\tilde{T}$ of the whole soil–structure system, which in this case is larger than in the corresponding no-rotation case by a factor of nearly 2†: for pier A21, $\tilde{T} \approx 1{\cdot}24$ *s*, compared with the 0·65 s value for A1; and for pier C21, $\tilde{T} \approx 0{\cdot}56$ s compared with the 0·35 s value for C1.

*It is of interest to note that C21 is the exact model of the failed bridge piers along the 600 m section of the Hanshin Expressway in Kobe, which collapsed in the 17 January 1995 earthquake

†If the superstructure were fixed at the pile cap (or soil surface) the increase, of course, would be by a factor of exactly 2

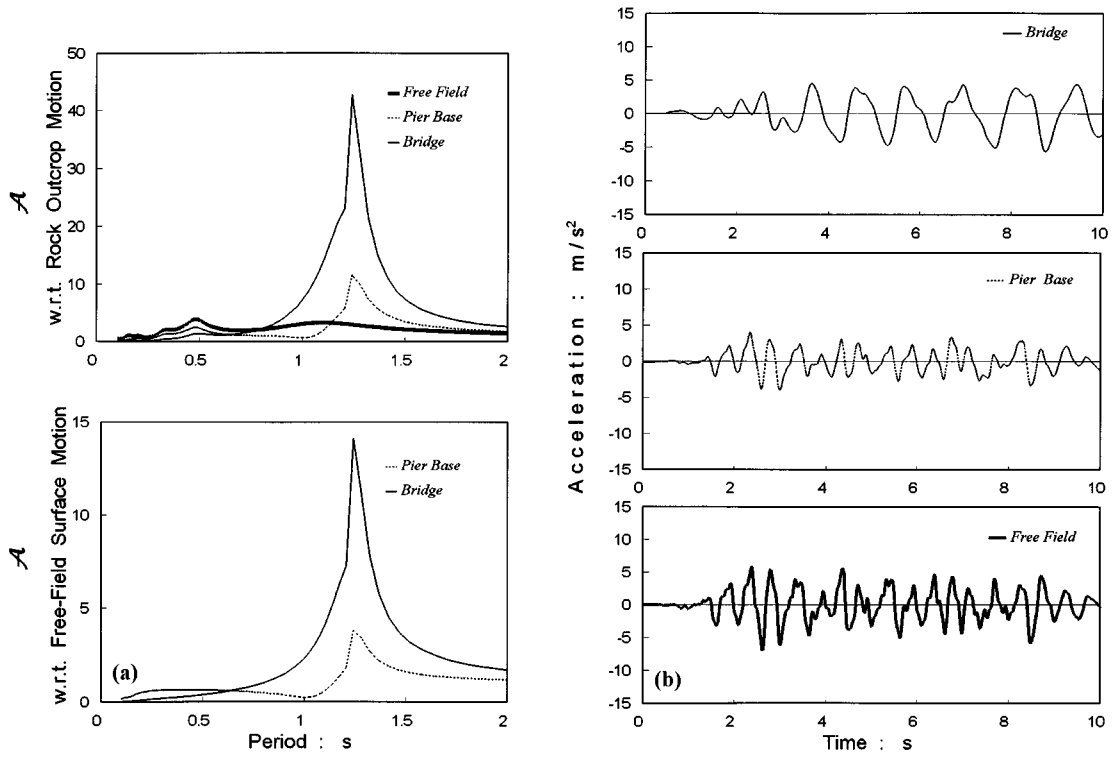

Figure 15. Case A21, column top free to rotate: results of the complete analysis in terms of: (a) harmonic steady-state transfer functions and (b) response acceleration histories for the artificial excitation

In both cases the amplification functions exhibit relatively sharp and high resonant peaks at periods $T = \tilde{T}$—sharper and higher than in the corresponding no-rotation cases. This may be attributed to three factors:

First, since the column top is in these cases free to rotate and move laterally, even a small rotation at the foundation level would lead to a large displacement at the top of the column, and hence to a larger amplification of the bridge motion.

Second, it just happened that the periods $\tilde{T}$ are closer, respectively, to either the fundamental (T_1) or the second (T_2) natural period of the soil deposit. Indeed, $T_1 \approx 1{\cdot}1$ *s* is relatively close to $\tilde{T} \approx 1{\cdot}25$ *s* (pier A21) and $T_2 \approx 0{\cdot}5$ s is relatively close to $\tilde{T} \approx 0{\cdot}56$ s (pier C21). Hence, we are closer to experiencing a double resonance in both 'free-to-rotate' cases.

Third, all the radiation damping of Pier A became zero at resonance ($T \approx \tilde{T} > T_1 = T_{\text{cutoff}}$). For pier C the radiation damping was also reduced, due to the fact that $T = \tilde{T} > T_2$ and T_2 is essentially a secondary cutoff period of the system.

In the time domain, despite the substantial increase in peak amplification, the bridge deck of pier A21 experiences only half the acceleration levels of A1. This is obvious due to the fact that the excitation is weak at long periods (1·25 s), and hence there is not much to amplify. Notice the dominant period of about 1·25 s in the bridge response time history.

By contrast, C21 experiences an acceleration very slightly higher than C1. In this case, the higher amplification barely outweighs the smaller spectral accelerations of the excitation.

Effect of ignoring pile radiation damping

To develop further insight to the problem and to assess the potential error from one of the frequently introduced approximations in practice, namely, ignoring pile radiation damping, we present Figures 17–18. They correspond to Piers A and C, respectively.

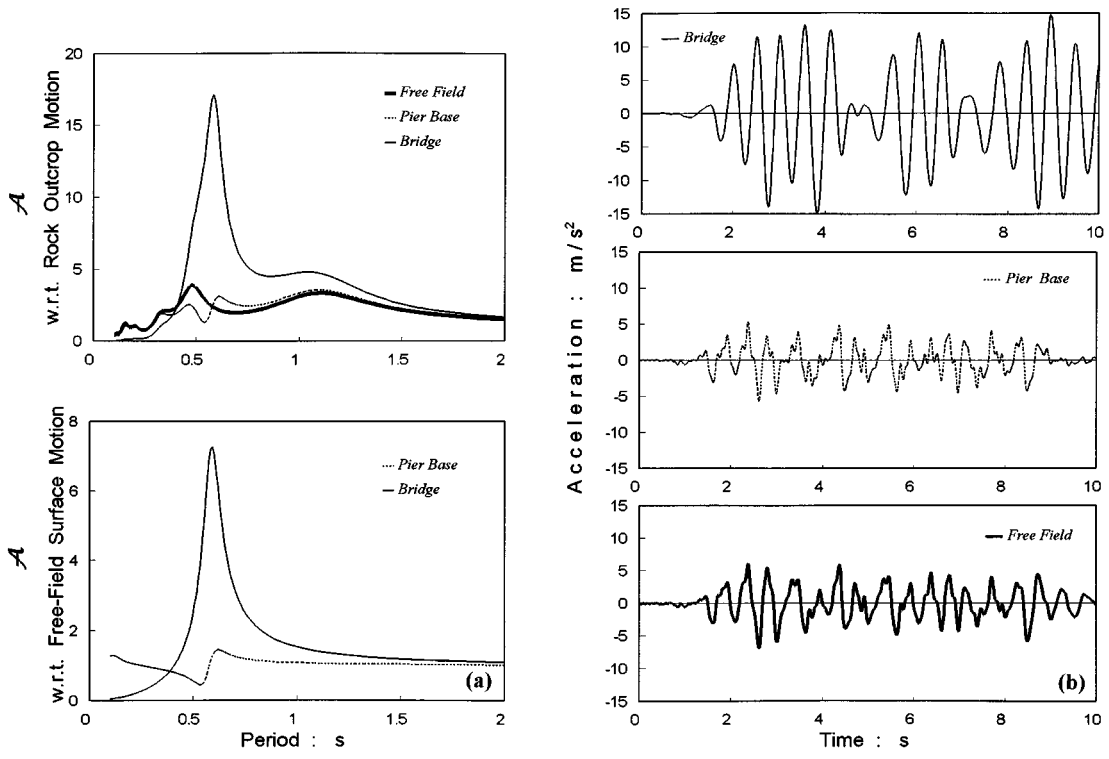

Figure 16. Case C21, column top free to rotate: results of the complete analysis in terms of: (a) harmonic steady-state transfer functions and (b) response acceleration histories for the artificial excitation

A large-diameter pile, e.g. with $d = 1{\cdot}30$ m, radiates significant amounts of energy when it oscillates laterally or vertically. This energy is carried from the pile periphery by radially spreading waves, propagating to infinity. In the dynamic impedance of the pile, such spreading away of the supplied by the pile energy is reflected (along with the hysteretic soil damping) in the dashpot constant C (equation (1)). With a group of piles, the radiation damping can at certain frequencies become dramatically larger than of the single pile, as a result of (additional) 'constructive interference' of the outward spreading waves.[56,38,39,59]

Indeed, the 'observed' resonant amplitudes at $T = \tilde{T}$ in the correct steady-state transfer functions with respect to free field (Figures 9 and 11) imply equivalent damping ratios greater than the assumed $\beta = 5\%$ structural damping of the pier column. Therefore, when radiation damping is (arbitrarily) set equal to zero, at all periods, the amplitudes at resonance increase substantially. In Figure 17, the two values of amplification $A(\tilde{T})$, with respect to rock outcrop and to free-field soil surface motion, double over the correct values of Figure 11. Since, however, the period $\tilde{T} = 0{\cdot}65$ s lies just beyond the range of dominant periods of the two excitation motions, the increase of the peak response accelerations is quite smaller: by a factor of 1·10 for the Pacoima (not shown) and of 1·40 for the artificial excitation. In both cases the dominant period of oscillation remains the same as that of the complete system. On the other hand, in Figure 18 (pile group), both $A(\tilde{T})$ values have increased by a factor of about 1·50. The acceleration histories reveal a change in the dominant response periods: The 0·35 s period is now more pronounced compared with the two periods in the complete solution (0·50 and 0·35 s). The increase of the peak acceleration amplitudes is approximately 10 per cent — again substantially less than the 50 per cent increase of the corresponding steady-state value. The relatively narrow width of the $A(T)$ curve at resonance might be the explanation of such discrepancy.

Finally, notice in Figure 14 that the bending moments change when pile radiation damping is set equal to zero. Specifically, whereas the kinematic moments at the clay–sand interface remain unchanged, the moments

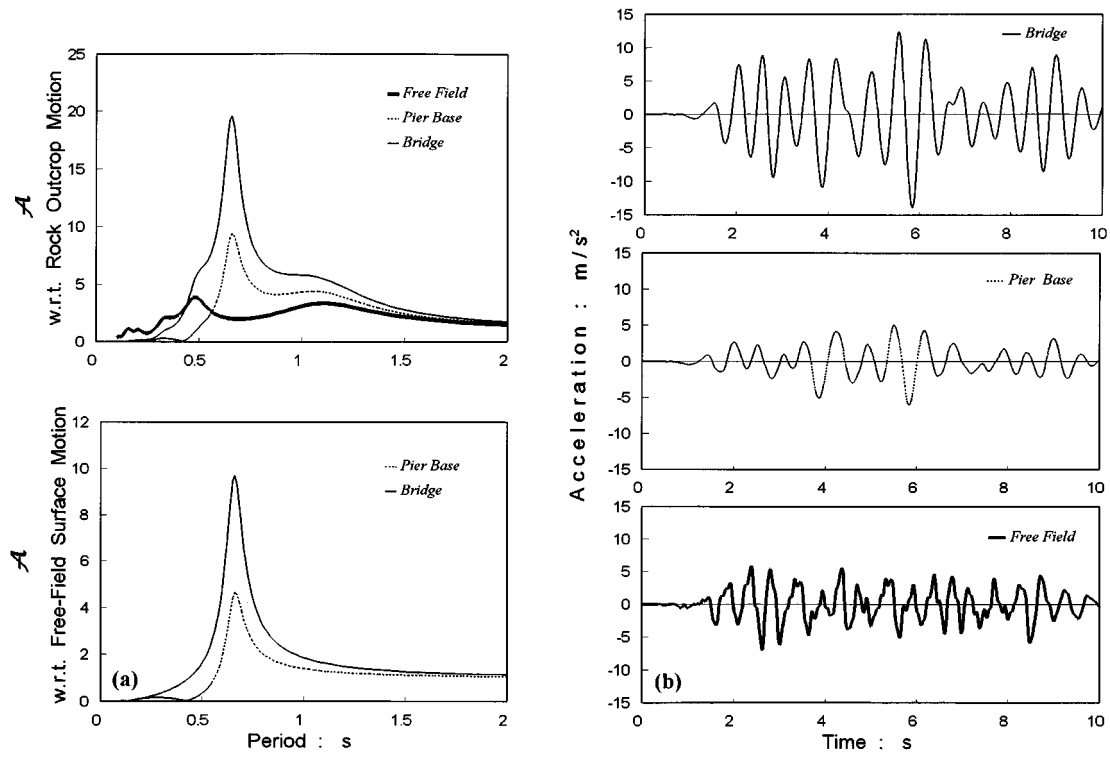

Figure 17. Case A4, no rotation at the column top, neglecting radiation damping: results in terms of: (a) harmonic steady-state transfer functions and (b) response acceleration histories for the artificial excitation

at the top increase by about 50 per cent in both cases studied (Piers A and C). This increase in moment diminishes with depth, vanishing at a depth equal to the '*active*' length of the pile ($l_a \approx 6$ and 12 m for the piles with 0·50 and 1·30 m diameter, respectively).

In conclusion, ignoring the radiation damping generated at the pile periphery leads to an overprediction of acceleration response at the bridge deck and pile bending moment, usually by not more than 50 per cent ('conservative' result). However, this should not be generalized to any bridge–foundation system.

Effect of ignoring foundation rotation

The rotational component of the motion at the base of the bridge (produced by both kinematic and inertial response) has been found to be significant primarily in the case of the single-pile foundations, such as the foundation of pier A, or footings with a very small number of piles. Any spurious fixity of this rotational degree of freedom will reduce the fundamental period and thereby change the dynamic response of the system.

This is illustrated herein with the help of Figure 19, which presents the steady-state and time-domain response of Pier A when no rotation is allowed to occur at the head of the pile. In this case the decrease of the period had a beneficial effect on the steady-state transfer function of the bridge response (peak of about 8·5 compared with the 9·8 of the correct solution of Figure 9)—apparently due to substantially increased radiation damping, once the period of the system became smaller (0·45 s) than T_2(0·5 s). Since, however, this shorter period ($\tilde{T} = 0{\cdot}45\ s$ compared with 0·65 s in Figure 9) falls in this case within the region of high spectral accelerations in the input motions, the time-domain acceleration exceeds the correct one by about 30 per cent. Similarly the pier base exhibits accelerations larger by about 40 per cent of the values of the correct motion.

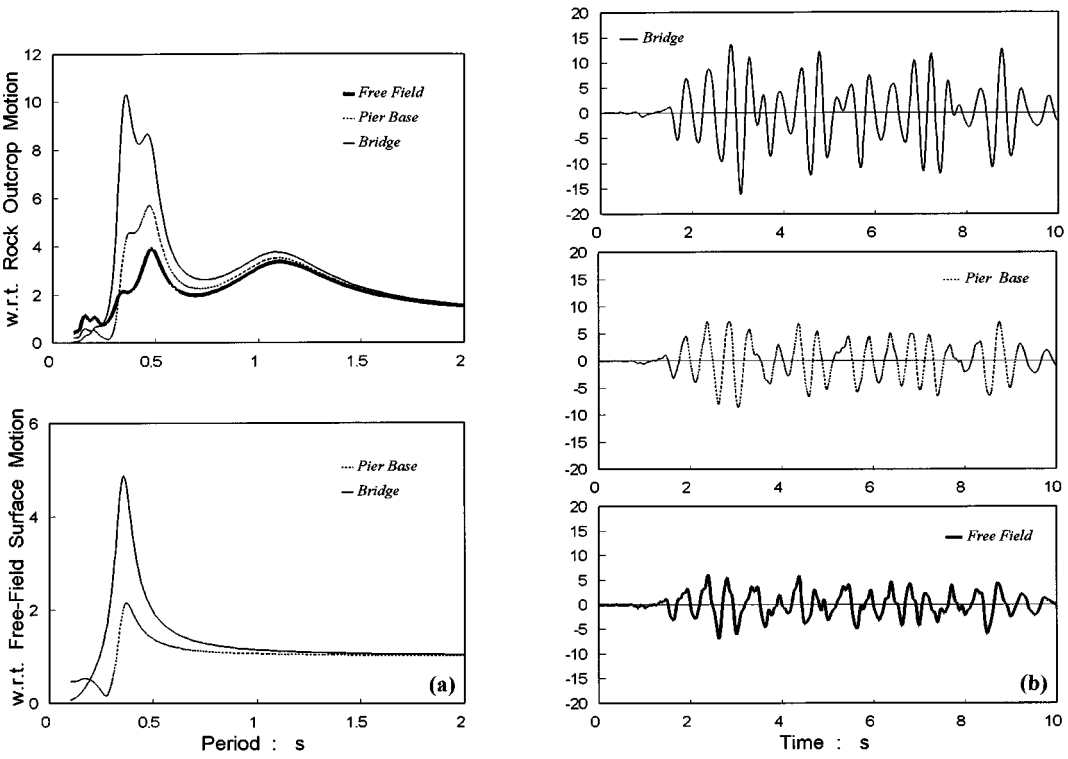

Figure 18. Case C4, no rotation at the column top, neglecting radiation damping: results in terms of: (a) harmonic steady-state transfer functions and (b) response acceleration histories for the artificial excitation

The rotational constraint provided by groups with a large number of piles renders the rocking component of foundation motion secondary. Consequently, ignoring foundation rotation would have a small effect on the response of the bridge or its foundation. No results of this effect are necessary to be shown here.

CONCLUSIONS, LIMITATIONS

The importance of soil–pile–structure interaction in the seismic behaviour of bridge piers is investigated with a multistep superposition procedure. Although the response seems to be influenced by a very large number of parameters, significant insight to the complicated mechanics of the problem has been developed from a parameter study involving two typical bridge piers in a realistic soft layered soil deposit excited by an artificial and an actual seismic rock motion.

The conclusions drawn from the parametric studies should not be generalized to bridge piers, soil deposits, and seismic excitations with characteristics vastly different from these of the studied cases. However, the observed phenomena and the discussed inertplay between the various natural periods of the system and the dominant periods of the ground excitation, can be of help in predicting qualitatively the response in other cases, or in interpreting the results of numerical studies.[60]

It is emphasized that the results presented in this paper are strictly applicable to (equivalent) linear soil and structure. Many of the quantitative results and some of the qualitative conclusions of the study might be modified considerably if strongly non-linear response were allowed to take place in the soil, the pile, or the superstructure. In bridge design (AASHTO[57]), such strong non-linearity is the rule for the superstructure ('ductility-based' design), while piles are designed to remain essentially elastic. With approximate techniques

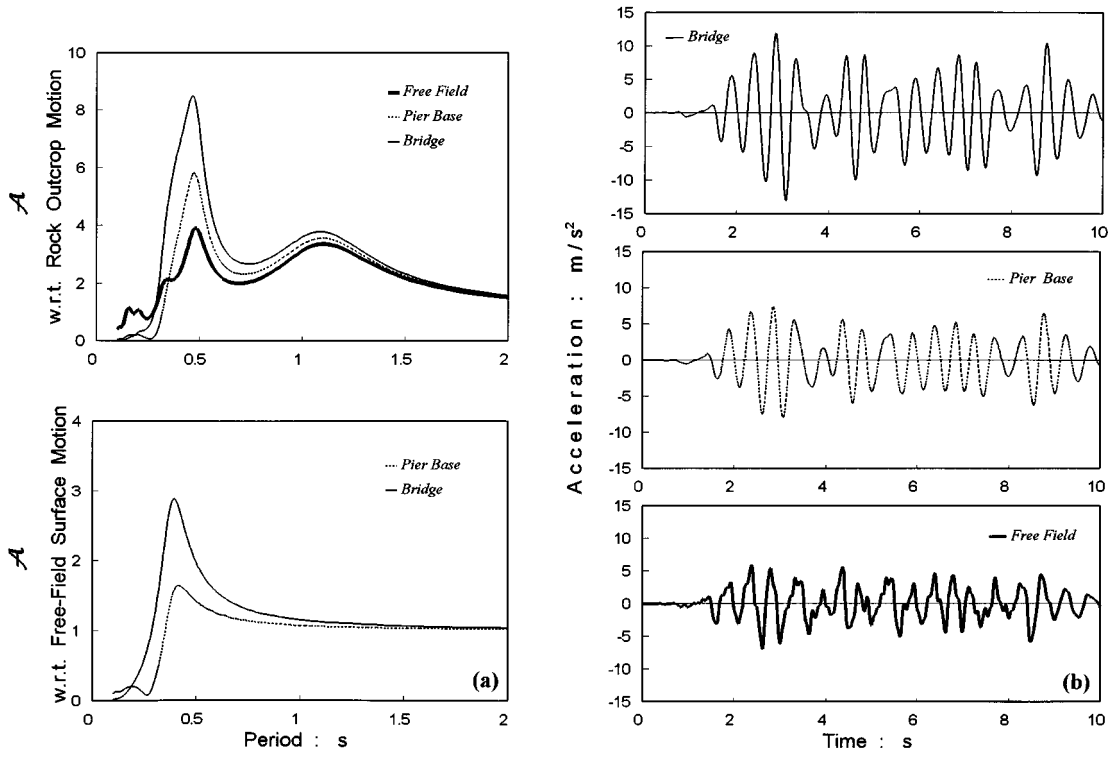

Figure 19. Case A3, no rotation at the column top, neglecting pile cap radiation: results in terms of: (a) harmonic steady-state transfer functions and (b) response acceleration histories for the artificial excitation

developed in structural dynamics,[41,58] only rough estimates of the inelastic structural response could be made using the equivalent-linear results of this study.

ACKNOWLEDGEMENTS

Funding for this work has been provided by: the National Center for Earthquake Engineering Research, by Shimizu Corporation, and by the EU Human Capital and Mobility Programme. We are Grateful for all this support.

REFERENCES

1. P. C. Jennings and J. Bielak, 'Dynamics of building–soil interaction', *Bull. seism. soc. Amer.* **63**, 9–48 (1973).
2. J. M. Roesset, R. V. Whitman and R. Dobry, 'Modal analysis for structures with foundation interaction', *J. struct. div. ASCE* **99**, 399–416 (1973).
3. A. S. Veletsos and J. W. Meek, 'Dynamic behaviour of building–foundation systems', *Earthq. eng. struct. dyn.* **3**, 121–138 (1974).
4. A. S. Veletsos, 'Dynamics of structure–foundation systems', in W. J. Hall (ed.), *Structural and Geotechnical Mech.*, Prentice-Hall, Englewood Cliffs, NJ, 1977.
5. J. Bielak, 'Modal analysis for building–soil interaction', *J. eng. mech. div. ASCE* **102**(EM5), 771–786 (1976).
6. J. Bielak 'Dynamic behaviour of structures with embedded foundations', *Earthquake eng. struct. dyn.* **3**, 259–274 (1975).
7. J. Lysmer, M. Tabatabaie, F. Tajirian, S. Vahdani and F. Ostadan, 'SASSI, a system for analysis of soil–structure interaction', *UCB/GT/81-02*, University of California, Berkeley, 1981.
8. J. E. Luco, 'Linear soil–structure interaction: a review', *Earthquake ground motion effects struct. ASME, AMD* **53**, 41–57 (1982).
9. J. P. Wolf, *Dynamic Soil–structure interaction*, Prentice-Hall, Englewood Cliffs, NJ, 1985.
10. J. Penzien 'Soil–pile foundation interaction', in R. L. Wiegel (eds.), *Earthquake Engineering*, Ch. 14, Prentice-Hall, Englewood Cliffs, NJ, 1970.
11. J. Bielak and V. J. Palencia, '*Dynamic behavior of structures with pile-supported foundations*', *Proc. WCEE*, New Delhi, 1977, pp. 1576–1581.
12. H. Takemiya and Y. Yamada, 'Layered soil–pile–structure dynamic interaction', *Earthquake eng. struct. dyn.* **9**, 437–458. (1981).

13. T. Tazoh, K. Shimizu and T. Wakahara, 'Seismic observations and analysis of grouped piles', *Dynamic Response of Pile Foundations-Experiment, Analysis and Observation, Geotechnical Special Publication, No. 11*, ASCE, 1987.
14. G. Gazetas, K. Fan, T. Tazoh, K. Shimizu, M. Kavvadas, and N. Makris, 'Seismic response of soil–pile–foundation–structure systems: some recent developments', in S. Prakash (ed.), *Piles Under Dynamic Loads, Geotech. Special Publ. No. 34, ASCE*, 1992, pp. 56–93.
15. ATC-3, *Tentative Provisions for the Development of Seismic regulations of buildings: a Cooperative Effort with the Design Profession, Building Code Interests, and the Research Community*', National Bureau of Standarts, Supt of Docs, Washington DC, 1978.
16. N. Makris and G. Gazetas 'Dynamic pile–soil–pile interaction. Part II: lateral and seismic response', *Earthquake eng. struct. dyn.* **21**, 145–162 (1992).
17. N. Makris, D. Badoni, E. Delis and G. Gazetas, 'Prediction of observed bridge response with soil–pile–structure interaction', *J. struct. eng. ASCE* **120**, 2992–3011 (1994).
18. M. Kavvadas and G. Gazetas, 'Kinematic seismic response and bending of free-head piles in layered soil', *Geotechnique* **43**, 207–222 (1993).
19. I. Lam and G. Martin, 'Seismic design of highway bridge foundation', *Report FHWA/RD-86/101 to Federal Highway Administration*, 1986.
20. G. M. Calvi and M. J. N. Priestley (eds), 'Seismic design and retrofitting of Reinforced concrete bridges', *Proc. Int. Workshop*, Bormio, Italy, April 2–5, 1991.
21. NEHRP, 'Recommended provisions for development of seismic regulations for new buildings', *Building Seismic Safety Council*, Washington, DC, 1991.
22. Eurocode EC8, 'Structures in seismic regions, Part 5: foundations, retaining structures, and geotechnical aspects', *First Draft, Brussels: Commision of the European Communities*, 1991.
23. G. Mylonakis, A. Nikolaou and G. Gazetas, 'Soil–pile–bridge seismic interaction: kinematic and inertial effects. Part II: stiff soil', 1997, submitted for publication.
24. G. Mylonakis, A. Nikolaou and G. Gazetas, 'Parametric results for seismic response of pile supported bridge bents', *NCEER-95-0021*, National Center for Earthquake Engineering Research, State University of New York, Buffalo, 1995.
25. G. Gazetas, G. Mylonakis and A. Nikolaou, 'Simple methods for the seismic response of piles applied to soil–pile–bridge interaction', *Proc. 3rd int. conf. on recent advances in geotechn. engng. soil dyn.*, St. Louis, Missouri, 1995.
26. E. Kausel and J. M. Roesset, 'Soil–structure interaction for nuclear containment structures', *Proc. ASCE*, Power Division Specialty Conf. Boulder, Colorado, 1994.
27. R. V. Whitman and J. Bielak, 'Foundations, design of earthquake resistant structures', E. Rosenblueth (ed.), Wiley, New York, 1980.
28. R. Flores-Berrones and R. V. Whitman, 'Seismic response of end-bearing piles', *J. geotech. eng. Div. ASCE* **108**, 554–569 (1982).
29. G. Gazetas, 'Seismic response of end-bearing piles', *Soil dyn. earthquake eng.* **3**, 82–93 (1984).
30. R. Dobry and M. J. O'Rourke, 'Discussion on seismic response of end-bearing piles' by Flores-Berrones, R. and Whitman, R. V., *J. geotech. eng. div. ASCE* **109** (1983).
31. M. Novak, 'Piles under dynamic loads: state of the art', *Proc. 2nd int. conf. on recent advances in geotech. earthquake engng and soil dyn.*, St. Louis, vol. 3, 1991, pp. 2433–2456.
32. M. Pender, 'Aseismic pile foundation design analysis', *Bull. New Zealand national soc. earthquake eng.* **26**, 49–160 (1993).
33. G. W. Blaney, E. Kausel and J. M. Roesset, 'Dynamic stiffness of piles', *Proc. 2nd int. conf. num. methods geomech.* Virginia Polytech. Inst. & State Un. Blacksburg VA II, 1976, pp. 1010–1012.
34. S. M. Mamoon and P. K. Banerjee, 'Response of piles and pile groups to travelling SH-waves', *Earthquake eng. struct. dyn.* **19**, (1990).
35. P. B. Schnabel, J. Lysmer and H. B. Seed, 'SHAKE: a computer program for earthquake response analysis of horizontally layered sites', *Report EERC 72-12*, University of California, Berkeley, 1972.
36. J. M. Roesset, 'Soil amplification of earthquakes', in C. S. Desai and J. T. Christian (eds.), *Numerical Methods in Geotechnical Engineering*, McGraw-Hill, New York, 1977.
37. A. S. Veletsos and C. E. Ventura, 'Efficient analysis of dynamic response of linear systems', *Earthquake eng. struct. dyn.* **12**, 521–536 (1984).
38. A. M. Kaynia and E. Kausel, 'Dynamic stiffness and seismic response of pile groups', *Research Report R82-03*, Massachusetts Inst. of Technology, 1982.
39. R. Dobry and G. Gazetas, 'Simple method for dynamic stiffness and damping of floating pile groups', *Geotechnique* **38**, 557–574 (1988).
40. W. T. Thomson, 'Transmission of elastic waves through a stratified solid medium', *J. appl. phys.* **21**, 89–93 (1950).
41. R. W. Clough and J. Penzien, *Dynamics of Structures*, Mc-Graw Hill, New York, 1975.
42. A. S. Veletsos, and K. W. Dotson, 'Impedances of soil layer with disturbed boundary zone', *J. geotech. eng.* **112** (1986).
43. K. W. Dotson and A. S. Veletsos, 'Vertical and torsional impedances for radially inhomogeneous viscoelastic soil layers', *Report. NCEER-87-0024*, National Center for Earthquake Engineering Research, State University of New York, Buffalo, 1987.
44. E. Chrysikou, 'Nonlinear dynamic analysis of axial pile vibration', *Diploma Thesis*, National Technical University of Athens, 1993.
45. G. Gazetas and R. Dobry, 'Horizontal response of piles in layered soil', *J. geotech. eng. div. ASCE* **110**, 20–40 (1984).
46. A. Nikolaou, G. Mylonakis and G. Gazetas, 'Kinematic bending moments in seismically stressed piles', *Report. NCEER-95-0022*, National Center for Earthquake Engineering Research, State University of New York, Buffalo, 1995.
47. M. Novak, 'Dynamic stiffnesses and damping of piles', *Canad. geotech. j.* **11**, 574–598 (1974).
48. G. Gazetas, 'Foundation vibrations' in *Foundation Engineering Handbook*, 2nd edn, Van Nostrand Reinholds, 1991, pp. 553–593.
49. I. Sanchez-Salinero, 'Dynamic stiffness of pile groups: approximate solutions', *Geotech. Engng. Rep.* GR83-5, Univ. Texas, Austin, 1983.
50. P. K. Banerjee and R. Sen, 'Dynamic behaviour of axially and laterally loaded piles and pile groups', in P. K. Banerjee and R. Butterfield (eds.), *Dynamic Behavior of Foundations and Buried Structures* (*Developments in Soil Mech. Found. Eng.*, Vol. 3), Elsevier App. Sc., London, pp. 95–133, 1981.
51. J. P. Wolf, *Simple Physical Models for Foundation Vibrations*, Prentice-Hall, Inc. Englewood Cliffs, NJ, 1994.

52. G. Gazetas, K. Fan, A. Kaynia and E. Kausel, 'Dynamic interaction factors for floating pile groups', *J. geotech. eng. div.*, ASCE, **117**, No. 10, 1531–1548 (1991).
53. H. El-Marsafawi, A. Kaynia, and M. Novak, 'Interaction factors and the superposition method for pile group dynamic analysis', *Report GEOT-1-92*, Geotechnical Research Center, Dept. of Civil Engineering, University of Western Ontario, Canada, 1992.
54. G. Mylonakis, 'Contributions to static and seismic analysis of piles and pile-supported bridge piers', *Ph.D. dissertation*, State University of New York at Buffalo, 1995.
55. R. Dobry, 'Soil properties and earthquake response', *Proc. X Europ. conf. soil mech. found. engng.*, Florence, vol. IV, 1994, pp. 1171–1189.
56. J. P. Wolf and G. A. Von Arx, 'Impedance function of a group of vertical piles', *Proc. specialty conf. on earthq. engng and soil dynamics*, ASCE, Pasadena, Calif., vol. 2, 1978, pp. 1024–1041.
57. AASHTO, '*Guide Specifications for Highway bridges*', Washinghton DC, 1983.
58. A. K. Chopra, *Dynamics of Structures*, Prentice-Hall, Englewood Cliffs, NJ, 1995.
59. T. Nogami, I. M. Idriss, M. S. Power and C. Y. Chang, 'Effect of radiation damping on earthquake response of pile-supported offshore platforms', *Earthquake eng. struct. dyn.* **11**, 337–353 (1982).
60. C. C. Spyrakos, 'Seismic behavior of bridge piers including soil–structure interaction', *Comput. & Struct.* **43**, 373–384.